Optica Applicata, Vol. XIX, No. 1, 1989

Third-order aberrations of the hologram realizing the Fourier transform process*

E. Jagoszewski, A. Talatinian**

Institute of Physics, Technical University of Wrocław, Wybrzeże Wyspiańskiego 27, 50-370 Wrocław, Poland.

The Fourier transform holographical element is presented. It has been shown that the hologram can be used as a Fourier transformer for determination of the spatial frequencies of an investigated object. For three different holograms, the third-order aberration coefficients are illustrated, and the deviation in the reconstructed wavefronts of several point objects is shown.

1. Introduction

The imaging properties of holograms are analogous to the lens properties in conventional imaging, therefore holography is sometimes called "lensless imaging". The focusing properties of a hologram have found many applications in various domains of science and technology. Analysis of the reconstructed waves shows that if the reconstructing source is situated at a position different from that of the reference source, the holographic image will occur at a position different from that of the object and will show aberrations. As we know, the focusing properties are used for the realizing of the optical Fourier transform [1].

In this paper, we show that a hologram recorded by the two waves: a spherical and a plane one, has the same effect in the reconstruction process as a thin lens in conventional collimating imagery. Therefore, the known paraxial positions of the holographic images (of an object point) reconstructed by a plane wave are given from the imaging lens formula. If the direction of this wave is parallel to the optical axis, then the images are the focal points of the hologram and determine its focal-planes. In the case of sloped reconstruction beams, we obtain the images in certain distance from the axis. Thus, the spatial frequencies of the object can be estimated.

2. Basic Fourier transform holographic model

It is known that a lens acts as a Fourier transformer of spatial distributions, providing the Fourier transform relationship between the amplitude in its front and back focal planes. In general, the Fourier transform relation between any object and

---

* This work has been sponsored by the CPBP 01.06 Research Programme.

** The author is with the University of Aleppo, Syria.

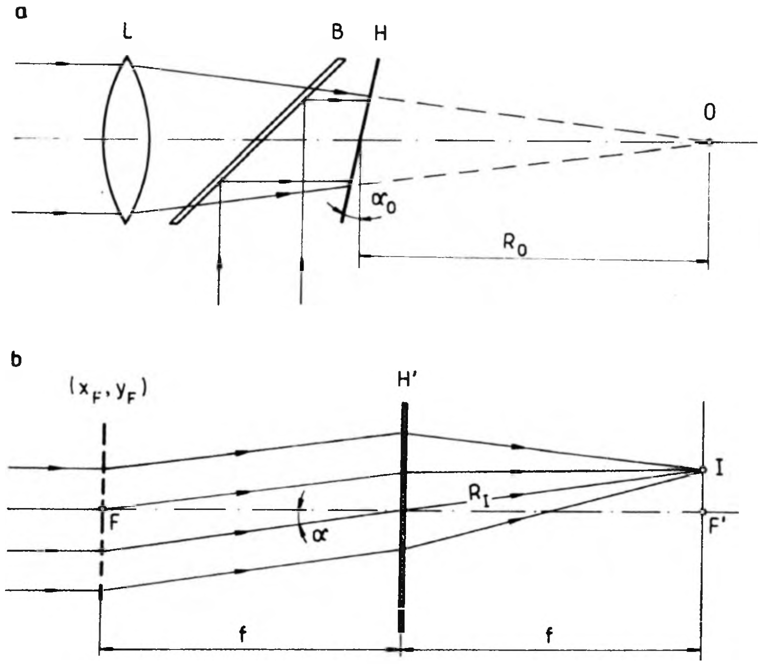

Fig. 1. Fourier transform holographic model: **a** — recording of a hologram. **b** — reconstruction process. L — lens, B — beam splitter, H — holographic plate, H' — hologram, O — object. I — image, F, F' — front and back focal points, respectively

the focal plane amplitude distribution of the lens is not an exact one, due to the presence of the quadratic phase factor. In this work, a hologram with the properties of a thin lens is considered, thus the reconstructed images (by a plane wave) provide to the Fourier transform of the investigated object. In Figure 1**a**, an optical system for producing of the hologram is shown. Figure 1**b** illustrates the plane wave of the complex amplitude distribution $u(x, y)$ incident at the hologram in the direction defined by the angle α. Thus, the amplitude distribution behind the hologram by assuming the infinite extent of its aperture becomes

$$u'(x,y) = u(x,y)\exp\left[-i\frac{k}{2R_I}(x^2+y^2)\right] \tag{1}$$

where R_I is the image distance from the middle of the hologram. If the reconstructing wavelength λ is equal to the wavelength λ_O of recording the hologram ($\mu = 1$), then the sloped (α_O) image beam forms an unaberrated point in the distance R_O at the back focal plane, and we have

$$u'(x,y) = u(x,y)\exp\left[-i\frac{k}{2f}(x^2+y^2)\cos\alpha_O\right]. \tag{2}$$

The imaging property of the hologram is characterized by its focal-length, which for the ray tracing in the x-z plane is defined by equation

$$f = R_O\cos\alpha_O,$$

where α_O is the inclination angle of the photographic plate during the hologram recording (Fig. 1**a**).

In this way, Figure 1**b** shows a system for the Fourier transform spatial realization of any amplitude distribution. Really, when the input amplitude is given in the front focal plane ($x_F - y_F$), then the wave propagates to the hologram, where after transforming by diffraction it runs again through the vacuum and illuminates the back focal plane, forming the Fourier transform of the input distribution. The fact is that the Fourier transform realization of the 2-D complex amplitude distribution has a practical matter in the optical image processing. It can be shown too, that if the object wave is sampled at a sufficiently large number of points, the discrete Fourier transform can be done with a computer program using the fast Fourier transform algorithm.

3. Aberrations of the Fourier spectrum

The model proposed here performs the Fourier transform relationship between two focal-planes of a point hologram. Therefore, we can use the CHAMPAGNE [2] formulation of the aberrations of image points in the back focal plane. Obviously, in one case, if the direction of the reconstructing wave coincides with the reference wave of this hologram, one can find an unaberrated image point which illustrates in the back focal plane one of the spatial frequencies of the input distribution [3], [4]. All of the next points are loaded with the aberrations. The wavefront deviation from the Gaussian reference sphere is then, as follows:

$$\Delta = -\frac{1}{2}\left[\frac{(x^2+y^2)^2 S}{4} - (x^2+y^2)(xC_x+yC_y)+(x^2A_x+y^2A_y+2xyA_xA_y)\right] \tag{3}$$

where x, y are the hologram coordinates, and S, C, A — the spherical aberration, coma and astigmatism coefficients, respectively, which in the theory of Champagne are written in the forms:

$$\begin{aligned}
S &= \frac{1}{R_C^3}-\frac{1}{R_I^3}\pm\mu\left(\frac{1}{R_O^3}-\frac{1}{R_R^3}\right),\\
C_x &= \frac{x_C}{R_C^3}-\frac{x_I}{R_I^3}\pm\mu\left(\frac{x_O}{R_O^3}-\frac{x_R}{R_R^3}\right),\\
C_y &= \frac{y_C}{R_C^3}-\frac{y_I}{R_I^3}\pm\mu\left(\frac{y_O}{R_O^3}-\frac{y_R}{R_R^3}\right),\\
A_x &= \frac{x_C^2}{R_C^3}-\frac{x_I^2}{R_I^3}\pm\mu\left(\frac{x_O^2}{R_O^3}-\frac{x_R^2}{R_R^3}\right),\\
A_y &= \frac{y_C^2}{R_C^3}-\frac{y_I^2}{R_I^3}\pm\mu\left(\frac{y_O^2}{R_O^3}-\frac{y_R^2}{R_R^3}\right),\\
\mathrm{A}_{xy} &= \frac{x_C y_C}{R_C^3}-\frac{x_I y_I}{R_I^3}\pm\mu\left(\frac{x_O y_O}{R_O^3}-\frac{x_R y_R}{R_R^3}\right).
\end{aligned} \tag{4}$$

Table 1. Spherical aberration ($10^7 S$)

α_1	0°	2°	4°	6°	8°	10°	12°	14°	16°	18°	20°
$\alpha_O = 0°$	0.00	+0.144	+0.573	+1.33	+2.31	+3.59	+5.13	+6.92	+8.94	+11.20	+13.60
$= 10°$	−3.59	−3.44	−3.01	−2.26	−1.28	0.00	+1.56	+3.33	+5.34	+7.58	+10.00
$= 20°$	−13.60	−13.50	−12.00	−12.30	−11.30	−10.00	−8.48	−6.71	−4.70	−2.45	0.00

Table 2. Coma ($10^5 C_x$)

α_1	0°	2°	4°	6°	8°	10°	12°	14°	16°	18°	20°
$\alpha_O = 0°$	0.00	−1.39	−2.78	−4.13	−5.46	−6.74	−7.96	−9.11	−10.20	−11.20	−12.10
$= 10°$	+6.74	+5.34	+3.96	+2.60	+1.28	0.00	−1.22	−2.37	−3.45	−4.44	−5.34
$= 20°$	+12.10	+10.70	+9.32	+7.97	+6.64	+5.36	+4.14	+2.99	+1.91	+0.898	0.00

Table 3. Astigmatism ($10^4 A_x$)

α_1	0°	2°	4°	6°	8°	10°	12°	14°	16°	18°	20°
$\alpha_O = 0°$	0.00	−0.243	−0.971	−2.17	−3.84	−5.94	−8.46	−11.40	−14.60	−18.20	−22.00
$= 10°$	+5.94	+5.70	+4.97	+3.77	+2.10	0.00	−2.52	−5.42	−8.67	−13.10	−16.90
$= 20°$	+22.00	+21.80	+21.00	+19.80	+18.20	+16.10	+13.50	+10.6	+7.39	+3.84	0.00

We note that when all the beams are only in the x-z plane then considerable simplification is possible, since the coefficients C_y, A_y and A_{xy} are zero. This reduction leads to three equations of aberrations, from which two of them are useful in the forms:

$$C_x = \frac{\sin\alpha_C}{R_C^2} - \frac{\sin\alpha_I}{R_I^2} \pm \mu\left(\frac{\sin\alpha_O}{R_O^2} - \frac{\sin\alpha_R}{R_R^2}\right),$$

$$A_x = \frac{\sin^2\alpha_C}{R_C} - \frac{\sin^2\alpha_I}{R_I} \pm \mu\left(\frac{\sin^2\alpha_O}{R_O} - \frac{\sin^2\alpha_R}{R_R}\right). \tag{5}$$

By specifying α and R of the image beam, we find the image point which is not necessary located with respect to the focal plane. Thus, we consider the aberrations in terms of imaging from a surface to the focal plane which include an unaberrated image point satisfying the Gaussian image formula. The other image points in the focal plane are loaded with the aberrations. Depending on how the hologram is recorded, we can obtain the unaberrated image for the on-axis or for the off-axis point. In our considerations we investigate rather the off-axis points representing the determined spatial frequencies of an actual object.

Let us examine three different holograms: two off-axis and one in-line hologram. For simplification all the beams by recording and reconstruction are in the x-z plane. Assuming the two recording beams: object and reference coaxial, the holograms of the focal-length $f = 50.000$ mm with $\alpha_O = 0°$, $10°$ and $20°$ are formed. In all three

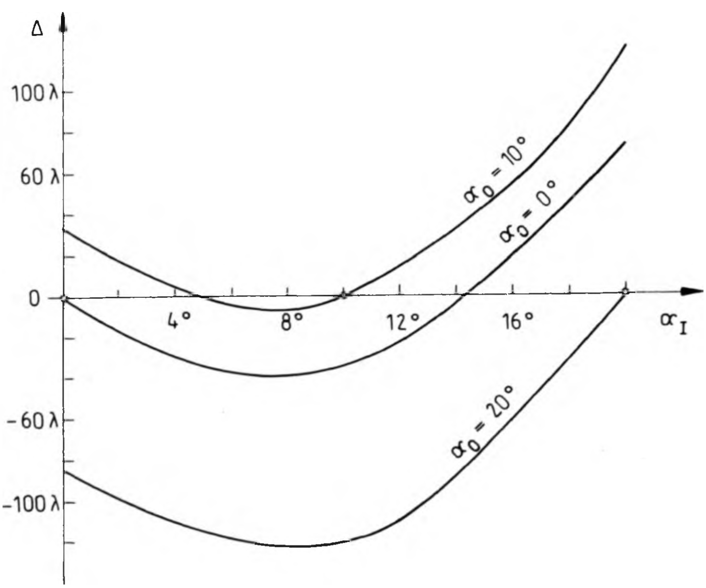

Fig. 2. Magnitude of the wavefront deviation vs the incident angle of the reconstruction beam for an in-line hologram ($\alpha_O = 0°$), and two off-axis holograms ($\alpha_O = 10°$, $20°$)

cases, we have an extended to 20° range of spatial frequencies. Corresponding to assumption, the reference and reconstruction waves are the plane ones, and equal to each other ($\mu = 1$). In Tables 1–3 one can find the values of the aberration coefficients: spherical aberration, coma and astigmatism, respectively. Applying Eq. (3), we obtain the wavefront deviation from the Gaussian reference sphere.

In this analysis, we have confined our attention to hologram f-number equals 2. Figure 2 illustrates the wavefront deviation in wavelength of $\lambda = 632.8$ nm for an in-line and the two off-axis holograms.

4. Conclusions

An in-line or off-axis point hologram can be used as a Fourier transformer of spatial distribution. It has been shown that if the incident angle of the recording beams is not large, then the solution can be satisfactory for a spatial frequency range of about 10°. In the presented considerations the best solution in the range from 3° to 12° of the spatial frequency values is for the $\alpha_O = 10°$ hologram.

References

[1] GOODMAN J. W., *Introduction to Fourier Optics*, McGraw-Hill, New York 1968.
[2] CHAMPAGNE E. B., J. Opt. Soc. Am. **57**, (1967), 51.
[3] WELFORD W. T., Opt. Commun. **8** (1973), 239.
[4] KEDMI J., FRIESEM A. A., Appl. Opt. **23** (1984), 4015.

Received September 12, 1988

Аберрации третьего порядка голограммы, реализующей операцию преобразования Фурье

Представлена голограмма как преобразователь Фурье. Было обнаружено, что плоская голограмма может быть использована для преобразования Фурье распределения амплитуды предмета и определения его простанственных частот. Для трех разных голограмм были проведены исследования аберрации третьего порядка и показано влияние геометрии системы на ошибки реконструированных волновых линий.